Neurotoxicology 75 (2019) 221–232

Contents lists available at ScienceDirect

Neurotoxicology

journal homepage: www.elsevier.com/locate/neuro

Full Length Article

IMM-H004 reduced okadaic acid-induced neurotoxicity by inhibiting Tau pathology *in vitro* and *in vivo*☆

Yingying Wang[a,b,1], Xiuyun Song[a,1], Dandan Liu[c], Yu-xia Lou[c], Piao Luo[d], Tianbi Zhu[d], Qi Wang[b,**], Naihong Chen[a,d,*]

[a] State Key Laboratory of Bioactive Substances and Functions of Natural Medicines, Institute of Materia Medica & Neuroscience Center, Chinese Academy of Medical Sciences and Peking Union Medical College, Beijing, 100050, China
[b] Guangzhou University of Chinese Medicine, Institute of Clinical Pharmacology, Guangzhou, 510405, China
[c] Tianjin University of Traditional Chinese Medicine, Tianjin, 300193, China
[d] Hunan University of Chinese Medicine, Changsha, 410208, Hunan, China

ARTICLE INFO

Keywords:
Alzheimer's disease
IMM-H004
Okadaic acid
Tau protein
Neuroprotection

ABSTRACT

This study aimed to explore effects and mechanisms of 004 (IMM-H004), a novel coumarin derivative, in OKA (okadaic acid)-induced AD (Alzheimer's disease)-like model. *In vitro*, MTT, LDH, and Annexin V/FITC flow cytometry assay were used to test cell survival. *In vivo*, OKA microinjection was conducted to simulate AD-like neuropathology. Morris water maze and Nissl staining were used to detect spatial memory function and neuronal damage respectively. Western blot and immunohistochemistry were used to study the mechanisms of 004 in Tau pathology. The results showed that 004 reduced cell death and increased survival in PC12 cells, and decreased neuronal injury in the hippocampus in rats. 004 improved learning and memory functions in OKA-treated rats. The mechanistic studies indicated that 004 inhibited phosphorylation of Tau protein by down-regulating the activity of protein kinases CDK5 and GSK3β and increasing PP2A activity. Overall, 004 improved spatial memory impairments and neuron cells injury induced by OKA; on the other hand, 004 inhibited Tau hyperphosphorylation by regulating CDK5, GSK3β and PP2A.

1. Introduction

As a common clinical neurodegenerative disease, AD is induced by complex factors, of which NFTs (neurofibrillary tangles) formed by hyperphosphorylation of Tau protein are one of the hallmarks in laboratory research (Martin et al., 2013, 2011). Tau is an important microtubule-associated protein that can regulate the assembly, dynamic behavior, and spatial organization of microtubules under physiological conditions (Medina and Avila, 2014). Under normal circumstances, protein kinases and protein phosphatases can maintain Tau protein at a physiological level. However, when the regulation of protein kinases and protein phosphatases changes, Tau protein and microtubules depolymerize, and abnormal accumulation of Tau hyperphosphorylation leads to formation of NFTs promotion of the AD process (Blennow et al., 2006; Martin et al., 2013).

Accumulating evidence suggests that the Tau protein phosphatase PP2A (protein phosphatase 2A, PP2A) and Tau protein kinases GSK-3β (glycogen synthase kinase-3β, GSK-3β) and CDK5 (Cyclin-dependent kinase-5, CDK5) are major regulators of Tau *in vitro and in vivo*. PP2A is one of the most significant serine/threonine phosphatases in the central nervous system. PP2A can regulate various signal transduction pathways, including cell cycle regulation, cell growth and development and cytoskeletal dynamics (Mo et al., 2014; Qian et al., 2010). The effect of Tau protein dephosphorylation is enhanced when PP2A activity is increased. Meanwhile, the activity of PP2A is decreased by abnormal hyperphosphorylation of Tau protein in the AD brain (Mo et al., 2014; Qian et al., 2010; Yang et al., 2016). CDK5 is a specific cell cycle-dependent kinase. Studies have shown that CDK5 can regulate a variety of

☆ Peer review under responsibility of Institute of Materia Medica, Chinese Academy of Medical Sciences and Peking Union Medical College.

* Corresponding author at: Institute of Materia Medica, Chinese Academy of Medical Sciences and Peking Union Medical College, Xiannongtan Street, Xuanwu District, Beijing, 100050, China.

** Corresponding author at: Institute of Clinical Pharmacology, Guangzhou University of Chinese Medicine, 12 Airport Road, Guangzhou, 510405, Guangdong Province, China.

E-mail addresses: wqitcm@qq.com (Q. Wang), chennh@imm.ac.cn (N. Chen).

[1] These authors contributed equally to this manuscript.

https://doi.org/10.1016/j.neuro.2019.09.012
Received 30 December 2018; Received in revised form 21 September 2019; Accepted 21 September 2019
Available online 25 September 2019
0161-813X/

substrates and play an important role in the development of the central nervous system. However, CDK5 activity also leads to the development of some neurodegenerative diseases, such as AD, under pathological conditions. For example, CDK5 can abnormally phosphorylate Tau protein and increase the formation of NFTs. Therefore, modulating the activity of CDK5 may be one strategy for the treatment of neurodegenerative diseases (Cruz and Tsai, 2004; Noble et al., 2003; Wilkaniec et al., 2016). GSK3β is a serine/threonine protein kinase that regulates the phosphorylation of serine/threonine residues in cytoplasmic proteins. As a major Tau protein kinase, GSK3β plays an important role in the process of AD by regulating Tau phosphorylation (Geschwind, 2003; Martinez et al., 2002; Wagner et al., 1996; Wang et al., 2015).

OKA is a specific protein phosphatase inhibitor that is mainly used to simulate AD-like lesions in the laboratory. Its main mechanism of action is the induction of phosphorylation abnormalities in a variety of microtubule-binding proteins, especially Tau protein, and NFT formation, resulting in changes in the neuronal cytoskeleton, eventually leading to cell death (Kamat et al., 2014, 2011). OKA induces the phosphorylation of Tau by inhibiting PP2A and activating CDK5 and GSK3β, thereby promoting the formation of intracellular NFTs (Kamat and Nath, 2015). Therefore, OKA was used as a neurotoxic agent to produce the AD model in our study.

Research has explored the roles of IMM-H004, [7-hydroxy-5-methoxy-4-methyl-3-(4-methylpiperazin-1-yl)-coumarin, 004, Fig. 1] in protecting against AD. Those results confirmed that 004 alleviates Aβ-induced neuronal injury (Song et al., 2013). Furthermore, administering 004 before OKA treatment inhibited abnormal Tau protein phosphorylation (Song et al., 2016a,b). These results indicated that 004 may be a promising compound for the prevention of OKA-induced AD-like degeneration. However, further studies are needed. Therefore, this study explored the therapeutic effect and the molecular mechanisms of 004 in OKA-induced AD-like degeneration. PP2A, CDK5 and GSK3β, which regulate the hyperphosphorylation of Tau protein, were explored in depth.

2. Materials

2.1. Cells and rats

PC12 cells, a common neural cell line, were purchased from ATCC (Maryland, USA) and maintained in Dulbecco's modified Eagle's medium (DMEM) supplemented with 5% fetal bovine serum (FBS) and 5% ES in an incubator at a constant temperature of 37 ℃ and 5% CO_2.

Adult male Sprague–Dawley (SD) rats (220 ± 20 g, 6–7 weeks old) from SPF Biotechnology Co., Ltd. (Beijing, China), were chosen for our experiments. All the rats were housed in a room and had free access to food and water and the housing conditions were at 23 ℃ and 12 h light/dark. All rats were handled according to the standards established in the Guide for the Care and Use of Laboratory Animals published by the Institute of Laboratory Animal Resources of the National Research Council (USA) and approved by the Animal Care Committee of the Peking Union Medical College and the Chinese Academy of Medical Sciences.

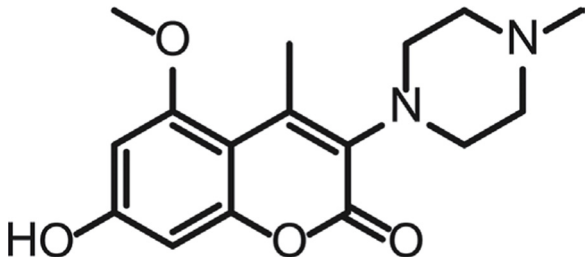

Fig. 1. The chemical structure of IMM-H004.

2.2. Compounds and reagents

OKA (okadaic acid, OKA) was purchased from Express Technology Co., Ltd. (Beijing, China), and 004 was obtained from Sphinx Scientific Lab Corporation (Tianjin, China). Melat (Melatonine, Melat) and DP (Donepezil, DP) were from the National Institutes for Food and Drug Control (Beijing, China).

The FITC Annexin V Apoptosis Detection Kit was purchased from BD (New Jersey, USA). The LDH Cytotoxicity Assay Kit was purchased from Beyotime Biotechnology Co., Ltd (Shanghai, China). The bicinchoninic acid (BCA) kit was obtained from Applygen Technologies (Beijing, China).

3. Methods

3.1. Cell viability

PC12 cells were cultured at density of 5×10^3/well (100 μL per well) in 96 well plates. Based on our preliminary study in PC12 cells, 30 nmol/l OKA was chosen as the most suitable model concentration (Wang et al., 2016). Subsequently, we explored the effect of 004 in the OKA model by MTT assays. The samples were divided into the Control, OKA, OKA + 004 (0.01 μM, 0.1 μM, 1 μM and 10 μM), and OKA + Melat (0.01 μM, 0.1 μM, 1 μM, and 10 μM) groups. OKA, 004 and Melat dissolved in DMSO (Dimethyl sulfoxide, DMSO) and Melat acted as positive control. The cell viability rate was detected after 36 h of incubation with OKA. MTT solution (0.5 mg/ml) was added to each well and the incubation was continued for 4 h at 37 ℃ in dark. Then samples were incubated with lysing buffer comprising 5% (v/v) isobutanol and 10% (g/v) sodium dodecyl sulfate for overnight at room temperature. The absorbance was measured at 570 nm.

3.2. Cell mortality

The LDH cytotoxicity assay kit was used. At 1 h before the end of drug treatment, we added the LDH release induction agent provided in the LDH cytotoxicity assay kit at a volume of 150 μL to the plate and mixed well. Then, the cells were incubated in the cell incubator for an additional 1 h. From each well, 120 μL of the supernatant was collected and placed in a new 96-well plate. Then, the samples were treated according to the instructions of the kit.

3.3. Flow cytometry to detect cell apoptosis/apoptosis analysis by Annexin V-FITC and PI staining

Annexin V-FITC staining precedes the loss of membrane integrity which accompanies the latest stages of cell death resulting from apoptotic. Cells are in early apoptosis are Annexin V-FITC positive and PI negative; and cells are in late apoptosis or already dead are both Annexin V-FITC and PI positive. (Chen et al., 2008).

To investigate whether 004 could reduce cell apoptosis, apoptosis was examined by flow cytometry. Following treatment, the cells were harvested, washed three times with ice-cold PBS, resuspended with 100 μL of binding buffer containing 5 μL of Annexin V-FITC, and incubated in the dark for 10 min. Then, the cells were resuspended with 5 μL of PI solution, and the cell suspension was diluted with 400 μL of binding buffer and then analyzed by flow cytometry after incubation for 10 min (BD, USA) (Vermes et al., 1995).

3.4. Microinjection and surgery

The rats were randomly assigned to 7 groups (n = 12). Microinjection was performed before drug administration, and rats were anesthetized with 300 mg/kg chloral hydrate intraperitoneally, except for the control rats, to perform the operation.

Rats in control group received no treatment. For the

microinjections, rats were anesthetized with chloral hydrate (300 mg/kg, ip) and restrained in a stereotactic apparatus (RWD, Shenzhen, China). The sham group was injected with 5 μL of saline, and the remainder of the rats (n = 60) were injected with OKA (diluted to 200 ng/5 μL with physiological saline after dissolved in absolute ethanol) into the right ventricle of brain, which was 0.8 mm anterior to Bregma, 1.5 mm to the right of the median line of the sagittal suture, and 3.6 mm ventral to the dura. Each rat (n = 72) received only one microinjection. The animals were injected *via* a transcranial route using a 10-μL Hamilton syringe fitted with a 26-gauge needle. And microinjection was completed before rat administration. The entire process of injection lasted for 5 min (5 μL/5 min); then, the needle was kept stationary for 5 min after the end of the injection. Finally, penicillin powder was applied around the wound and rats were sutured immediately after the syringe was removed.

3.5. Morris water maze

We chose the Morris water maze training system to assess spatial learning and memory, as has been described in detail previously for rats (Song et al., 2016a,b). Two sites were selected for the navigation and spatial exploration experiments, and we calculated the mean escape latency and number of platform crossings (Vorhees and Williams, 2006).

The rats were divided randomly into control group, sham group, OKA group, DP (1 mg/kg) + OKA group, compound 004 (2, 4 and 8 mg/kg) + OKA group. 004 and DP administered by intragastric administration once daily at 8 a.m. on the day after microinjection and trained in the Morris water maze. 004 and DP dissolved in distilled water and DP acted as positive control. The dose of donepezil was determined by conversion of the regular dose for humans to that for rats (Stoiljkovic et al., 2018; Zheng et al., 2018). There were two tests, the orientation navigation and spatial probe tests, in our Morris water maze experiment. As shown in Fig. 2, the Morris water maze experiment was conducted from the 15th to the 18th day of drug administration. All rats were placed in the first quadrant or the fourth quadrant facing the pool wall. Animals unable to locate the target platform were guided to it, and the maximal latency time recorded was 120 s. On the 19th day, the spatial exploration experiment was carried out: the target platform (in the second quadrant) was removed, and each rat was placed in the water in the first quadrant. The number of times the rats passed through the region of the original target platform, the residence time and the average speed of the rats were recorded.

3.6. Nissl staining and immunohistochemistry

On the 21 st day, four rats randomly chosen from each group were anesthetized with chloral hydrate (300 mg/kg, *i.p.*) and perfused with 0.1 mol/L PBS (pH 7.4) followed by 4% paraformaldehyde in PBS. Then, the brains were removed and stored in 4% paraformaldehyde for more than 24 h. The brain tissues throughout the hippocampus were cut into 4-μm-thick coronal sections for immunohistochemistry after dehydration and subsequent embedding in paraffin blocks. In the Nissl staining experiment, the paraffin sections were incubated with Nissl staining solution (centrifuged to remove impurities before use) after treatment according to the literature for 1 h at room temperature (Huang et al., 2013). Then, the sections were washed twice in distilled water, dehydrated twice in 90% alcohol, incubated twice in fresh xylol, and then coverslipped with 90% glycerinum (Zhou et al., 2013).

In the immunohistochemistry experiment, the slices were incubated overnight at 4 °C with a primary antibody (1:200) after blocking with 5% BSA, followed by incubation with the corresponding secondary antibody (1:200) for 1 h at room temperature. After washing 3 times with PBST, the samples were dyed with 3,3′-diaminobenzidine (DAB) substrate. The dye staining was observed using a microscope. Then, the slices were dehydrated with an alcohol gradient (80%, 90%, and 100%), cleared, and coverslipped with neutral resin adhesive.

3.7. Western blot

Cell and tissue samples (four rats randomly chosen from each group and the maximum deviation one was eliminated in the statistics) were quantified using the BCA protein assay kit. The samples were separated by sodium dodecyl sulfate (SDS)-polyacrylamide gel electrophoresis (PAGE) in a 12% gel and electroblotted onto a PVDF membrane. After blocking with 3% bovine serum albumin in Tris buffer, the membrane was incubated overnight at 4 °C with antibodies specific for GSK-3α/β (Cell Signaling Technology Cat# 5676, RRID:AB_10547140), Phospho-GSK-3α/β (Tyr 216) (Santa Cruz Biotechnology Cat# sc-81496, RRID:AB_1125866), Phospho-GSK-3-beta (Ser9) (Cell Signaling Technology Cat# 9322S, RRID:AB_2115196), Anti-beta Actin (Abcam Cat# ab8226, RRID:AB_306371), Tau Monoclonal Antibody (TAU-5) (Thermo Fisher Scientific Cat# MA5-12808, RRID:AB_10980631), Phospho-Tau pSer214 (Thermo Fisher Scientific Cat# 44–742 G, RRID:AB_2533740), Phospho-Tau pThr212 (Thermo Fisher Scientific Cat# 44–740 G, RRID:AB_2533739), Phospho-Tau pThr181 (Thermo Fisher Scientific Cat# 701530, RRID:AB_2532491), Phospho-Tau pThr205 (Thermo Fisher Scientific Cat# 44–738 G, RRID:AB_2533738),

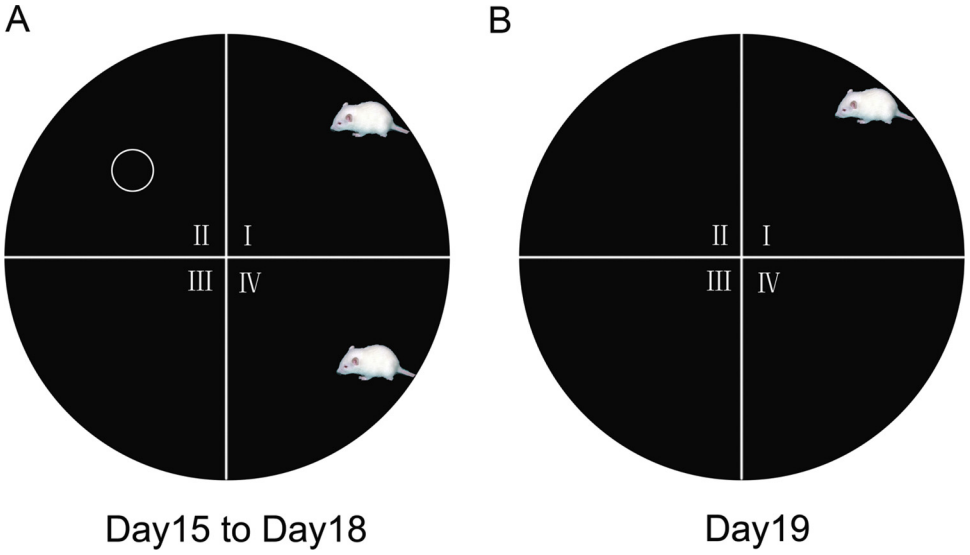

Fig. 2. Schematic diagram of the Morris water maze experiment of SD rats. A: In the orientation navigation test, from day 15 to day 18, the target platform was in the second quadrant, and all rats were placed in the water from the first quadrant or the fourth quadrant. Then, we intercalated that the navigation time was 120 s, and once each rat reached the platform, the rat was allowed to stay on the target platform for 30 s. B: In the spatial probe test, the target platform was removed, and all rats were placed in the water from the first quadrant.

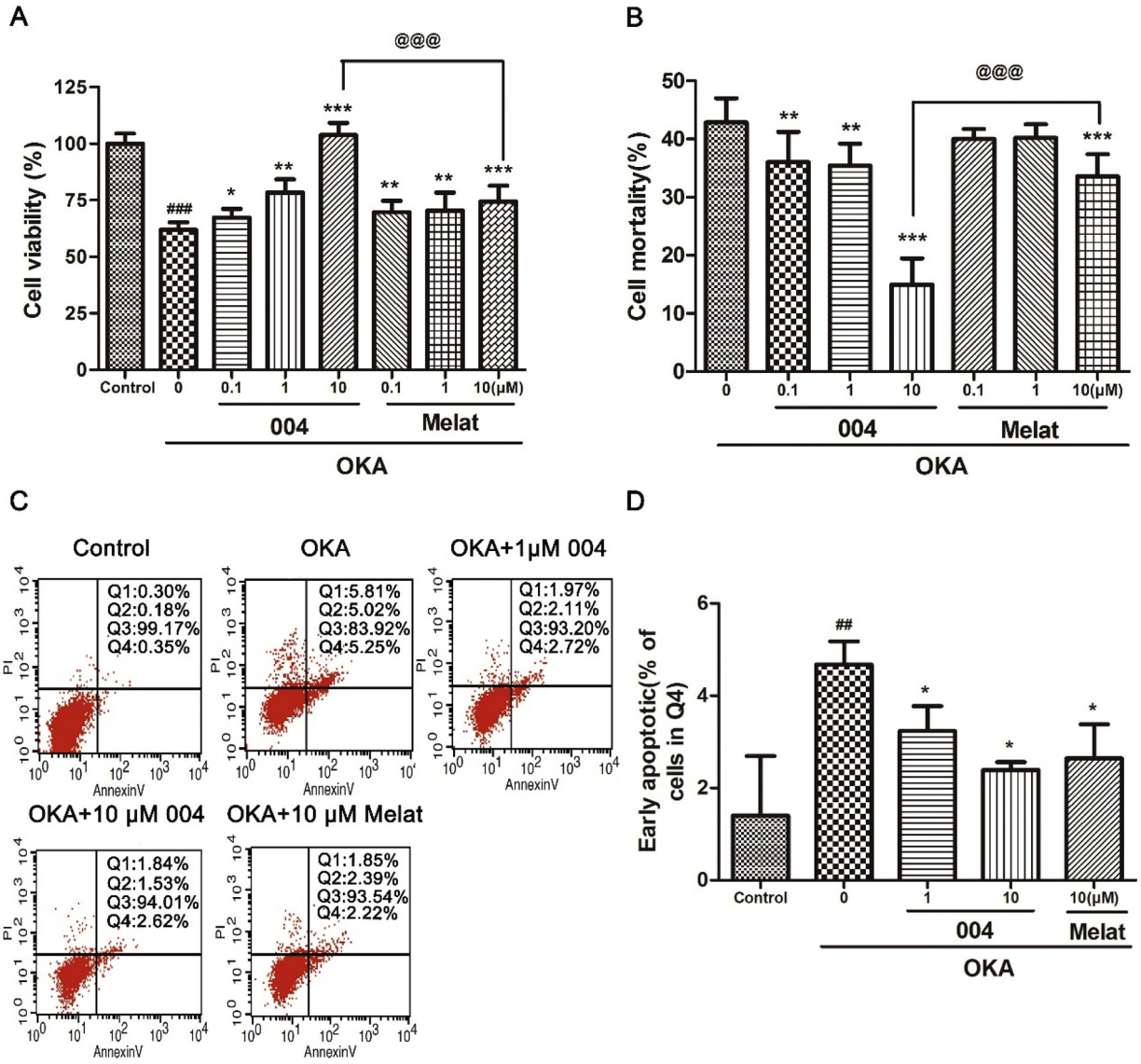

Fig. 3. 004 inhibited early apoptosis of PC12 cells induced by OKA. A: The results of MTT assays show that 004 significantly improved the cell survival rate. B: The results showed that 004 decreases the cell death rate based on the level of intracellular LDH. C: 004 significantly decreased early apoptosis (the percentage of cells in Q4) by OKA of cells based on flow cytometry. D: OKA significantly increased early apoptosis (the percentage of cells in Q4) induced by OKA compared with Control, 004 and Melat significantly decreased early apoptosis. Q1: Late apoptosis cells, Q2: Dead cells, Q3: Viable cells, Q4: Early apoptosis cells. $^{\#\#}p < 0.01$, $^{\#\#\#}p < 0.001$ *vs.* the Control group; $^{*}p < 0.05$, $^{**}p < 0.01$, $^{***}p < 0.001$ *vs.* the OKA group; $^{@@@}p < 0.001$, the 10 μM 004 group *vs.* the 10 μM Melat group. Mean ± SD in each group, n = 3.

Phospho-Tau (Thr231) (Thermo Fisher Scientific Cat# 701056, RRID:AB_2532360), CDK5 Antibody (Thermo Fisher Scientific Cat# MA5-11291, RRID:AB_10979358) according to the experimental needs. After washing with TBST 3 times, the membrane was incubated with the corresponding secondary antibody (1:5000) for approximately 2 h at room temperature. The immunoreactive bands were visualized by enhanced chemiluminescence after washing with TBST and were quantified with Quantity One software (Quantity One 1-D Analysis Software, RRID: SCR_014280).

3.8. The protein phosphatase activity assay for PP2A

PP2A activity in the cell and tissue extracts was detected according to the manufacturer's protocol (V2460 kit, Promega, USA), and cell and rat tissue samples were prepared according to previous reports (Bialojan and Takai, 1988; Reszka Krzysztof and Britigan Bradley, 2007; Zhao et al., 1993). Endogenous free phosphates were removed, and the protein contents of the cell and tissue extracts were normalized across all samples using a BCA protein assay kit. Samples were incubated with reaction premix solutions in a 96-well plate (provided in the kit) for 30 min at 30 °C. The reaction was stopped by adding 50 μL of molybdate dye/additive mixture. Then, we detected the release of phosphate by measuring the optical density of the malachite green-phosphomolybdate complex using a plate reader with a 630 nm filter (Reszka Krzysztof and Britigan Bradley, 2007).

4. Statistical analysis

The GraphPad Prism 5.0 (Graphpad Prism, RRID: SCR_002798) software package was used to analyze the quantitative data. All data are presented as the means ± SD except for the data from the Morris water maze and Western blot assays (the standard deviation is too large and the results from both assays were presented as the means ± SEM). Data were analyzed by ANOVA followed by Newman-Keuls Multiple Comparison Test. *A P*-value < 0.05 was considered statistically significant.

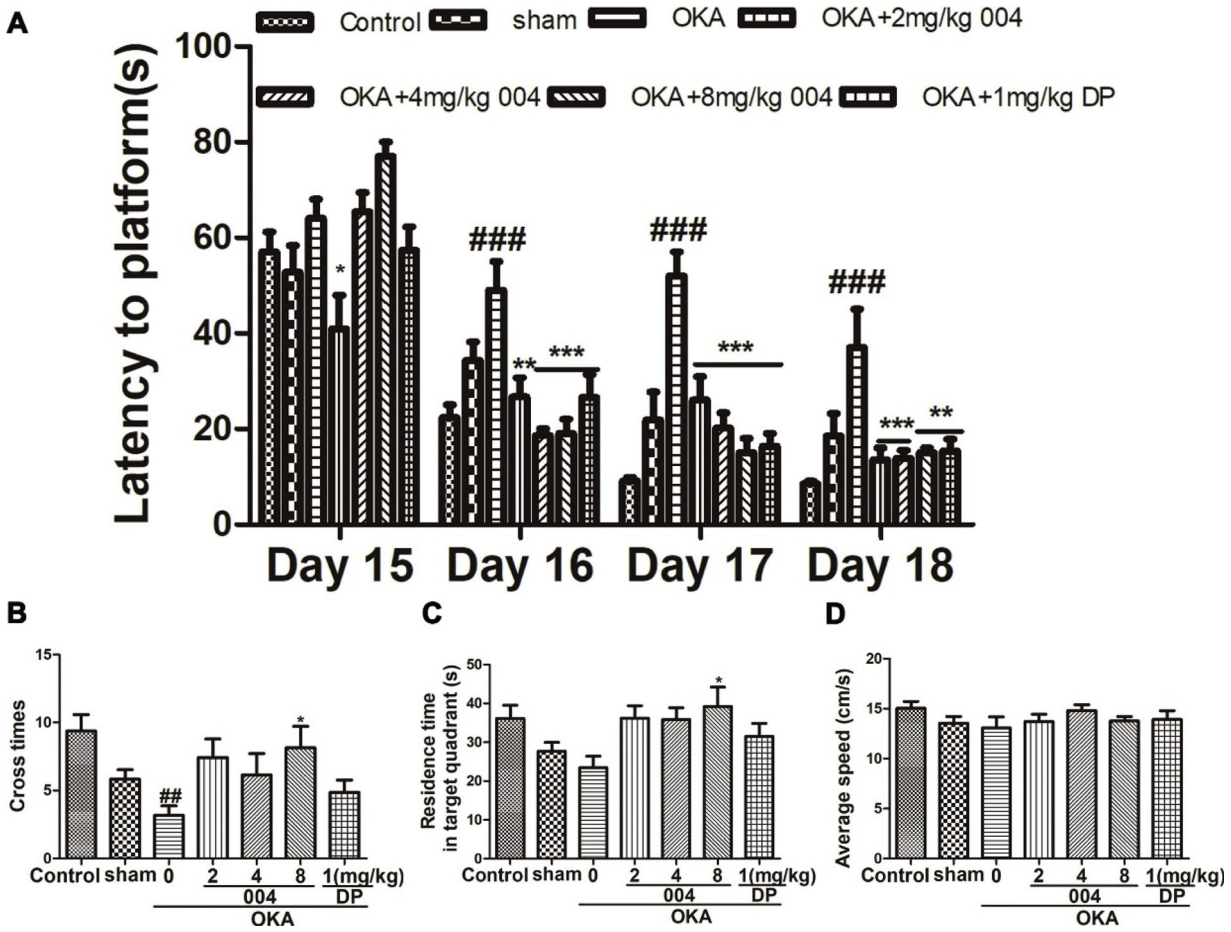

Fig. 4. 004 alleviated the deficits in learning and memory induced by OKA injection in rats. A: The escape latency of rats; B: number of platform crossings; C: the residence time of the rats on the platform; D: the average speed of the rats in each group, the average speed in each group was not significantly affected. DP acted as positive control in all data. $^{\#\#}p < 0.01$, $^{\#\#\#}p < 0.001$ *vs.* the Control group; $^{*}p < 0.05$, $^{**}p < 0.01$, $^{***}p < 0.001$ *vs.* the OKA group. mean ± SEM in each group, n = 8–12.

5. Results

5.1. 004 inhibited the apoptosis of PC12 cells induced by OKA

MTT and LDH assays were used to test cell viability and cell mortality. As shown in Fig. 3A and B, OKA significantly decreased cell viability, increasing the percentage of dead PC12 cells. 004 or Melat treatment improved the number of cells alive in a dose-dependent manner. Importantly the effect of 004 was stronger than that of Melat at the same dose.

Apoptosis is a normal physiologic process that occurs during embryonic development (Vermes et al., 1995). We measured the effect of 004 on the early apoptosis of PC12 cells by flow cytometry. As shown in Fig. 3C and D, cell apoptosis in the OKA group was significantly higher than that in the control group ($p < 0.01$), and cells treated with 004 + OKA and Melat + OKA had a lower early apoptosis rate than cells treated with OKA alone ($p < 0.05$). These results suggested that 004 and Melat inhibited early apoptosis induced by OKA.

These results confirmed that 004 suppresses the toxicity of OKA by inhibiting cell apoptosis and improving cell survival.

5.2. 004 reduced OKA-induced learning and memory dysfunction in rats

The Morris water maze, which is often used to examine learning and memory function in the setting of AD, was used in our experiment. In the learning stage, from days 15 to 18, the escape latencies were recorded. The results showed that (Fig. 4A) the escape latency was prolonged significantly in the OKA group compared with the Control group and the Sham group. In contrast, the escape latency from day 15 to day 18 was significantly shortened by treatment with 004 and DP. On day 19, we removed the platform, and the number of crosses over the platform location was significantly different between the Control and OKA groups; there was a significant decrease in platform crossings in the OKA group ($p < 0.01$). The number of platform crossings increased significantly *via* treatment with 8 mg/kg 004 ($p < 0.05$) (Fig. 4B). The residence time (Fig. 4C) showed a significant improvement trend only between the OKA group and the 8 mg/kg 004 + OKA group ($p < 0.05$). However, there was no statistical significance among the OKA, Control and Sham groups. It may be due to the small sample size and the large individual differences among rats. In addition, the swimming speed did not vary significantly among groups on day 19 (Fig. 4D). Based on the above results, we confirmed that the escape latency was significantly prolonged in rats after OKA injection. In addition, compared with the Control group, the number of platform crossings was significantly reduced in rats in the OKA group, suggesting that OKA induced spatial memory impairment. In contrast, 004 and DP significantly reduced the escape latency. Moreover, the number of platform crossings was increased significantly in the rats in the 8 mg/kg 004 group, suggesting that 004 and DP attenuated the spatial memory impairment induced by OKA. These behavioral test results indicated that OKA certainly damaged the spatial memory of rats and that 004 or DP prevented this impairment induced by OKA. Overall, these results provided support for the subsequent experiments.

For a more intuitive view, the Nissl staining method was used to

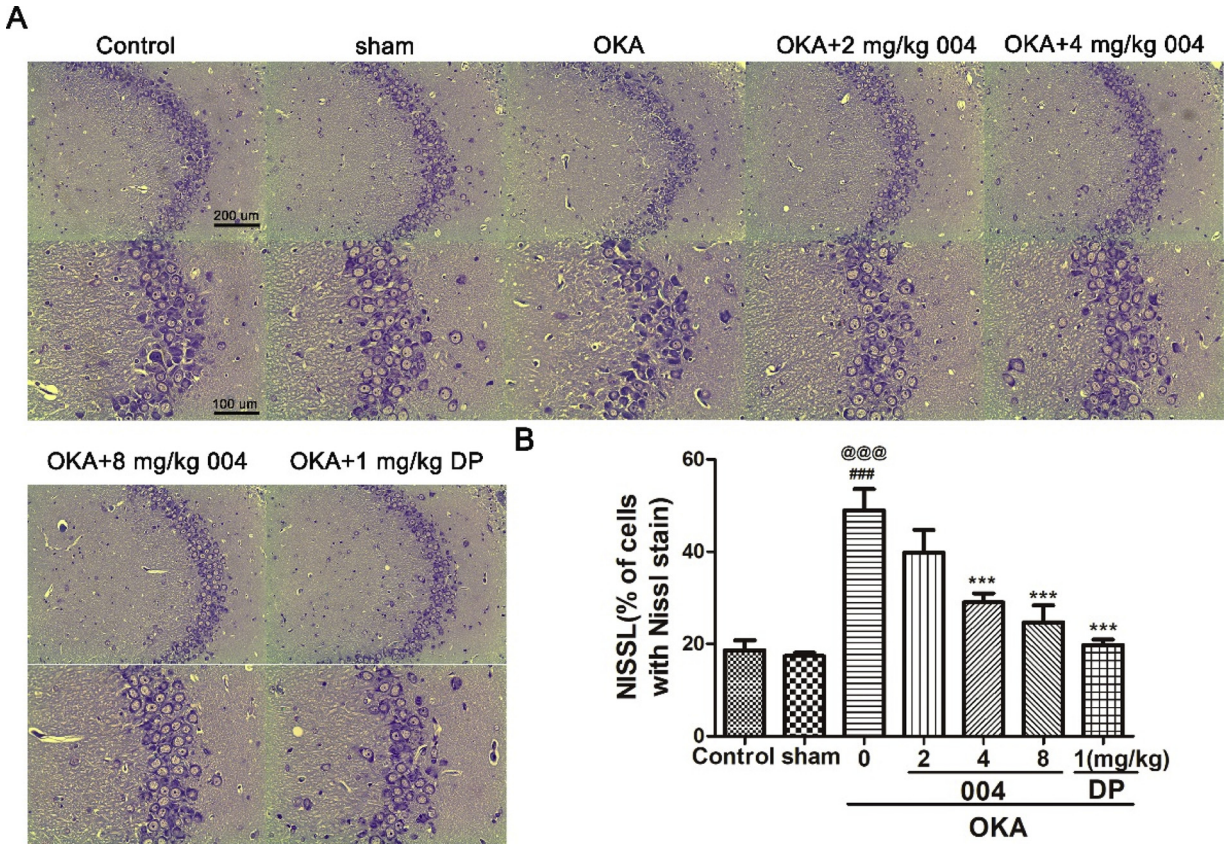

Fig. 5. 004 inhibited OKA-induced neuronal apoptosis in the CA3 region of the hippocampus in rats. A: Nissl staining in the CA3 region of the right hippocampus. OKA induced neuronal apoptosis, and 004 or DP significantly reduced the apoptosis of hippocampal neurons. $^{###}p < 0.001$ *vs.* the Control group; $^{@@@}p < 0.001$ *vs.* the Sham group; $^{***}p < 0.001$ *vs.* the OKA group. Mean ± SD in each group, n = 4. Ordinates represent the percentage of damaged (trachychromatic) neurons among all neurons per unit area.

validate the above results. The Nissl staining results showed (Fig. 5A) that hippocampal neurons in CA3 (the right hippocampus of rats was chosen in our experiment) in the OKA group were darkly stained and reduced in number with shriveled nuclei compared with hippocampal neurons in the Control group and the Sham group ($p < 0.001$), suggesting that OKA induced hippocampal neuronal apoptosis. After treatment with 004 and DP, the above phenomena were significantly alleviated ($p < 0.001$), suggesting that 004 and DP significantly suppressed the OKA-induced apoptosis of hippocampal neurons (Fig. 5B). The above results were obtained by calculating the percentage of apoptotic hippocampal neurons among all neurons per unit area.

The results of the behavioral studies and Nissl staining indicated that OKA injection induced the dysfunction of learning and memory and apoptosis of hippocampal neurons, while 004 or DP played an important role in improving learning and memory function and inhibiting the apoptosis of hippocampal neurons induced by OKA and exerted a neuroprotective effect. This evidence provided a basis for the study of the mechanism of the protective effect of 004 in AD.

5.3. 004 decreased Tau hyperphosphorylation by modulating the protein phosphatase PP2A and the protein kinases CDK5 and GSK3β

Firstly, we tested some Tau phosphorylation sites. Putative phosphorylation sites on the Tau protein were chosen for detection in our experiment, including S214, T212, T205, T181, and T231 (Alonso et al., 2010; Simic et al., 2016). According to the results, we observed that Tau sites S214 (Fig. 6A and B) and T231 (Fig. 6A and C) were hyperphosphorylated after OKA treatment compared with the control treatment *in vitro* ($p < 0.01$). Additionally, 004 and Melat decreased the phosphorylation level of Tau by regulating S214 and T231 phosphorylation *in vitro* ($p < 0.05$, $p < 0.01$). There were four Tau phosphorylation sites, S214, T205, T231, and T181, with significant hyperphosphorylation in the OKA group compared with the Control and Sham groups ($p < 0.05$ and $p < 0.01$, respectively) *in vivo*, indicating that OKA intervention induced Tau protein hyperphosphorylation at sites S214, T231, T205 and T181. In contrast, 004 down-regulated the phosphorylation level of Tau at sites S214, T205, T231 and T181 (Fig. 6D–H). These results indicated that 004 reversed the Tau pathology induced by OKA *in vitro and in vivo*.

To verify the above results further and in an intuitive fashion, we used immunohistochemistry in the following experiment, and we chose Tau sites S214 and T231 (both of which showed significant changes in phosphorylation levels), as shown in Fig. 7A (S214), the Control and Sham groups showed weak staining of S214 in the right CA3 region. However, staining of S214 was stronger in rats with OKA injection than in sham-treated rats. T231 staining showed the same alterations (Fig. 7B). However, 004 treatment at different doses significantly reversed these alterations. Nevertheless, the DP group showed no difference in Tau phosphorylation compared with the OKA group, similar to the results from Western blot analysis. These results suggested that 004 attenuated the hyperphosphorylation of Tau induced by OKA *in vitro* and *in vivo*.

Next, Western blot was used to detect the levels of the kinases CDK5 and GSK3β and the Tau phosphorylation levels at different Tau sites *in vitro* and *in vivo*. The results (Fig. 8) showed that the level of CDK5 increased significantly in the OKA group compared with the Control group both in PC12 cells and in rats. 004 and Melat administration decreased CDK5 levels greatly *in vitro*. Furthermore, 004 and DP had played the same effect *in vivo*. These results suggested that OKA upregulated CDK5 both *in vitro* and *in vivo*. In addition, 004 decreased the

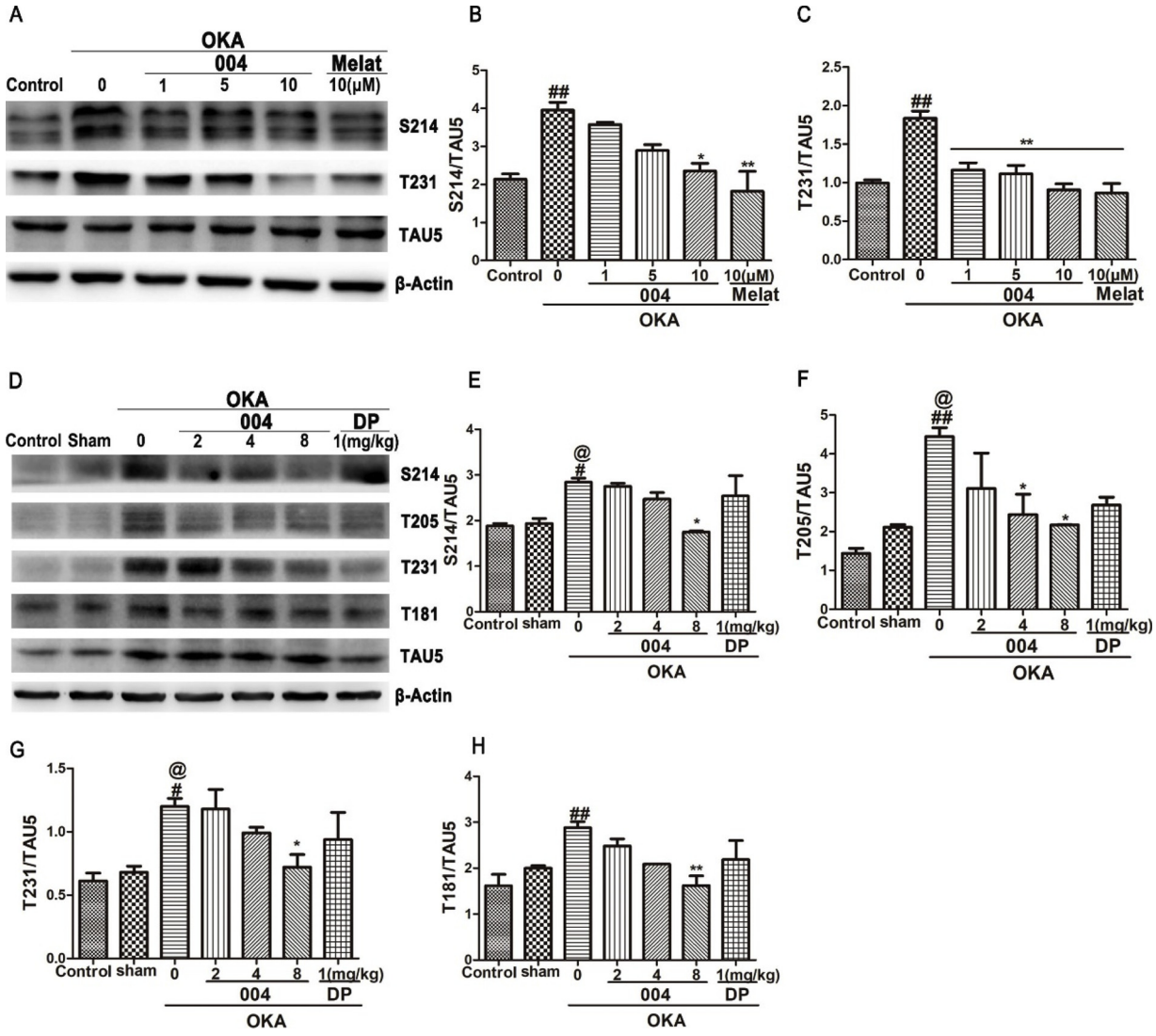

Fig. 6. 004 reversed the Tau pathology induced by OKA *in vitro* and *in vivo*. A and B: Western blot shows that 004 prevented PC12 cell death by regulating Tau phosphorylation at site S214, which was hyperphosphorylated in the presence of OKA; A and C: 004 decreased the level of Tau phosphorylation at site T231 in PC12 cells. D and E: 004 decreased the level of Tau phosphorylation at site S214 in rats. D and F: 004 decreased the level of Tau phosphorylation at site T205 in rats. D and G: 004 decreased the level of Tau phosphorylation at site T231 in rats. D and H: 004 decreased the level of Tau phosphorylation at site T181 in rats. $^{\#}p < 0.05$, $^{\#\#}p < 0.01$ *vs*. the Control group; $^{@}p < 0.05$ *vs*. the Sham group; $^{*}p < 0.05$, $^{**}p < 0.01$ *vs*. the OKA group. Mean ± SEM in each group.

level of CDK5. Moreover, the level of GSK3β in the OKA group was increased significantly compared with the Control group *in vitro*; however, the 004 (10 μM) group had greatly reduced GSK3β levels ($p < 0.01$). Then, we measured S9 and T216 phosphorylation of GSK3β. The results indicated that OKA treatment significantly decreased GSK3β S9 phosphorylation ($p < 0.01$) and increased T216 phosphorylation ($p < 0.05$) both *in vitro* and *in vivo*. The results also showed that 004 administration increased the phosphorylation of GSK3β at S9 and decreased phosphorylation of GSK3β at T216, which suggested that 004 inhibited GSK3β activity by modulating its phosphorylation at S9 and T216 *in vitro* and *in vivo*.

Finally, a PP2A activity assay kit was used to determine the effect of 004 on the activity of PP2A. As shown in Fig. 9A, PP2A activity was decreased significantly in PC12 cells incubated with OKA ($p < 0.05$). However, the 004 (10 μM) and Melat (10 μM) groups showed significantly enhanced PP2A activity ($p < 0.01$), suggesting that these compounds increased PP2A activity in PC12 cells. A similar result was observed in rats (Fig. 9B). These results suggested that 004 enhanced PP2A activity in the OKA-induced AD model *in vitro* and *in vivo*.

6. Discussion

NFTs, which are mainly composed of abnormally phosphorylated Tau protein, are hallmarks of AD in laboratory research (Martin et al., 2013, 2011). Tau hyperphosphorylation in Alzheimer's disease leads to sequestration of Tau and other microtubule-associated proteins, which causes disaggregation of microtubules and thus harms axonal transport, thereby impairing neuronal and synaptic function (Blennow et al., 2006; Medina and Avila, 2014). In AD, Tau phosphorylation results in the formation of NFTs (Blennow et al., 2006). The results of our study indicated that 004 treatment alleviated spatial memory impairments and inhibited brain cell apoptosis induced by OKA in rats and inhibited apoptosis in PC12 cells.

In AD, OKA treatment in the brain leads to mitochondrial dysfunction and increased protein expression of caspase-3, Bad, and Bax (Kamat et al., 2014, 2011; Yoon et al., 2006), and previous reports indicate that OKA could be an important inducer of apoptosis (Kamat et al., 2014). In our experiment, our results confirmed that 004 increased cell viability and suppressed neuronal apoptosis. And 004 ameliorated the deficits in learning and memory function induced by

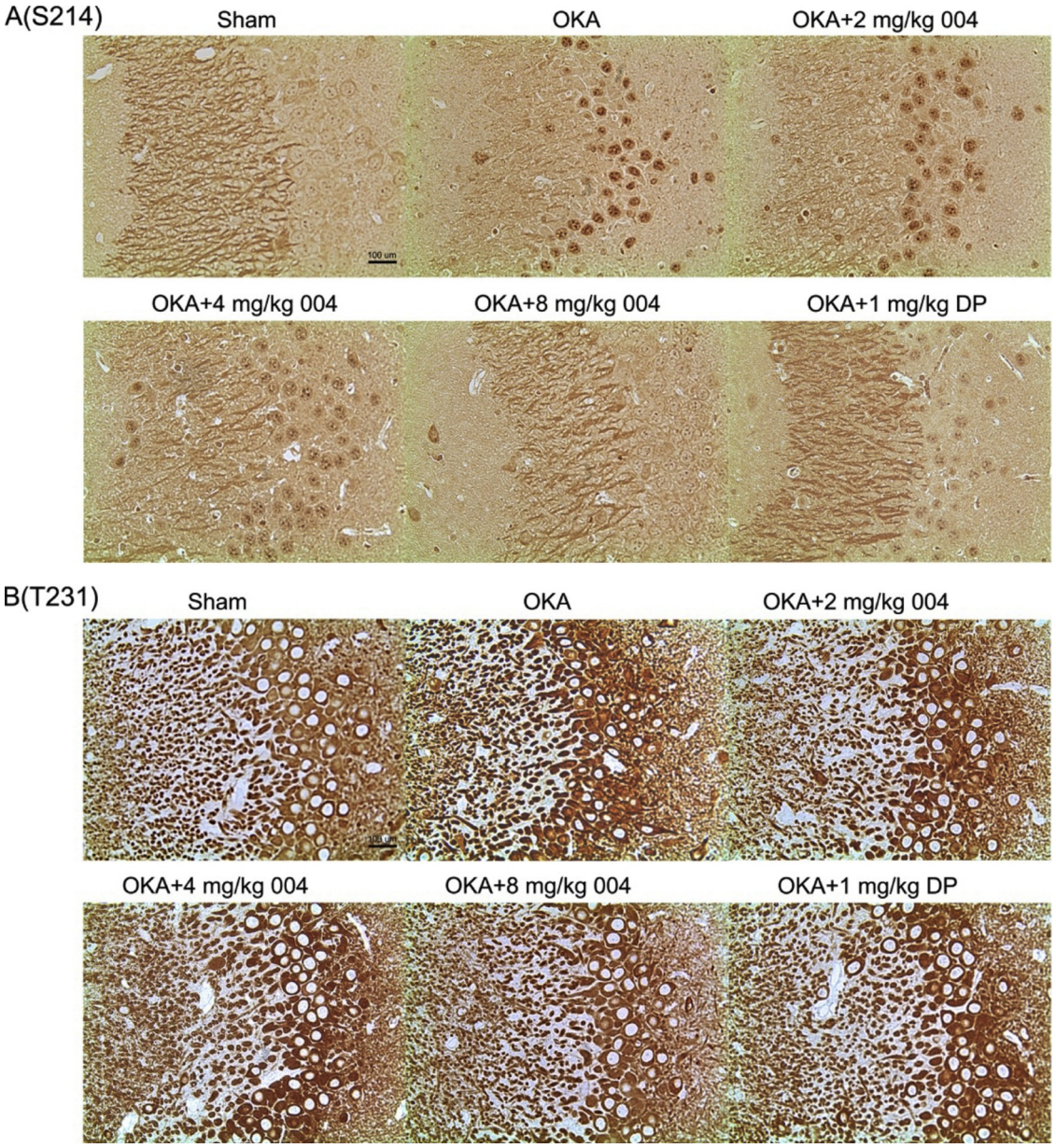

Fig. 7. Immunohistochemical staining of Tau protein phosphorylation at sites S214 and T231. A: Staining of phosphorylated Tau at S214 in the right CA3 region of rats; B: Staining of phosphorylated Tau at S214 in the right CA3 region of rats. There are no statistical results.

OKA.

Based on previous studies, it is well known that Tau is a member of the family of microtubule-associated proteins, which an important role in the assembly of tubulin monomers into microtubules to constitute the neuronal microtubule network (Martin et al., 2013, 2011; Medina and Avila, 2014). Abnormally phosphorylated Tau is a major neuropathological hallmark of tauopathies, including AD (Geschwind, 2003). Previous studies have shown that different Tau kinases and phosphatases induce distinct catalytic effects on different Tau sites and that CDK5 can directly phosphorylate Tau at T212 and T205 (Alonso et al., 2010; Simic et al., 2016). Tau site T205 is the favored phosphorylation site for PP2A, while S214 is less favored; Tau sites T205 and T231 are target sites for GSK3β, while T181 and S262/356 are less favored sites, although there is a difference between *in vitro* and *in vivo* results (Liu et al., 2007; Longin et al., 2007; Wang et al., 2015). In our results, there were obvious fluctuations in the Tau phosphorylation levels at S214, T231, T205 and T181, but there was no significant difference in Tau phosphorylation at T212. We demonstrated that 004 reversed the neurotoxicity of abnormally phosphorylated Tau induced by OKA both *in vitro* and *in vivo*.

PP2A, CDK5 and GSK3β play important roles in the phosphorylation and dephosphorylation of Tau. They are major Tau phosphatases and kinases *in vitro* and *in vivo* (Buée et al., 2000). PP2A is apparently the most active enzyme in dephosphorylating abnormally hyperphosphorylated Tau to a normal-like state (Wang et al., 1995, 1996). In the AD brain, the activity of PP2A is decreased. When PP2A is inhibited *in vitro* or *in vivo*, Tau is hyperphosphorylated at several sites (Gong et al., 2000; Liu and Wang, 2009; Tanaka et al., 1998). Tau is phosphorylated by several protein kinases, such as CDK5 and GSK3β. Both CDK5 and GSK3β are proline-regulated protein kinases that mainly act on the proline-linked serine/threonine residues of Tau (Tian et al., 2004). Increasing evidence indicates that CDK5 deregulation promotes the neurodegenerative pathogenesis of AD by regulating a series of intracellular signaling pathways. CDK5 activity is confirmed to lead to intracellular accumulation of hyperphosphorylated Tau protein in NFTs (Song et al., 2016a,b). GSK3β is also a key enzyme involved in the

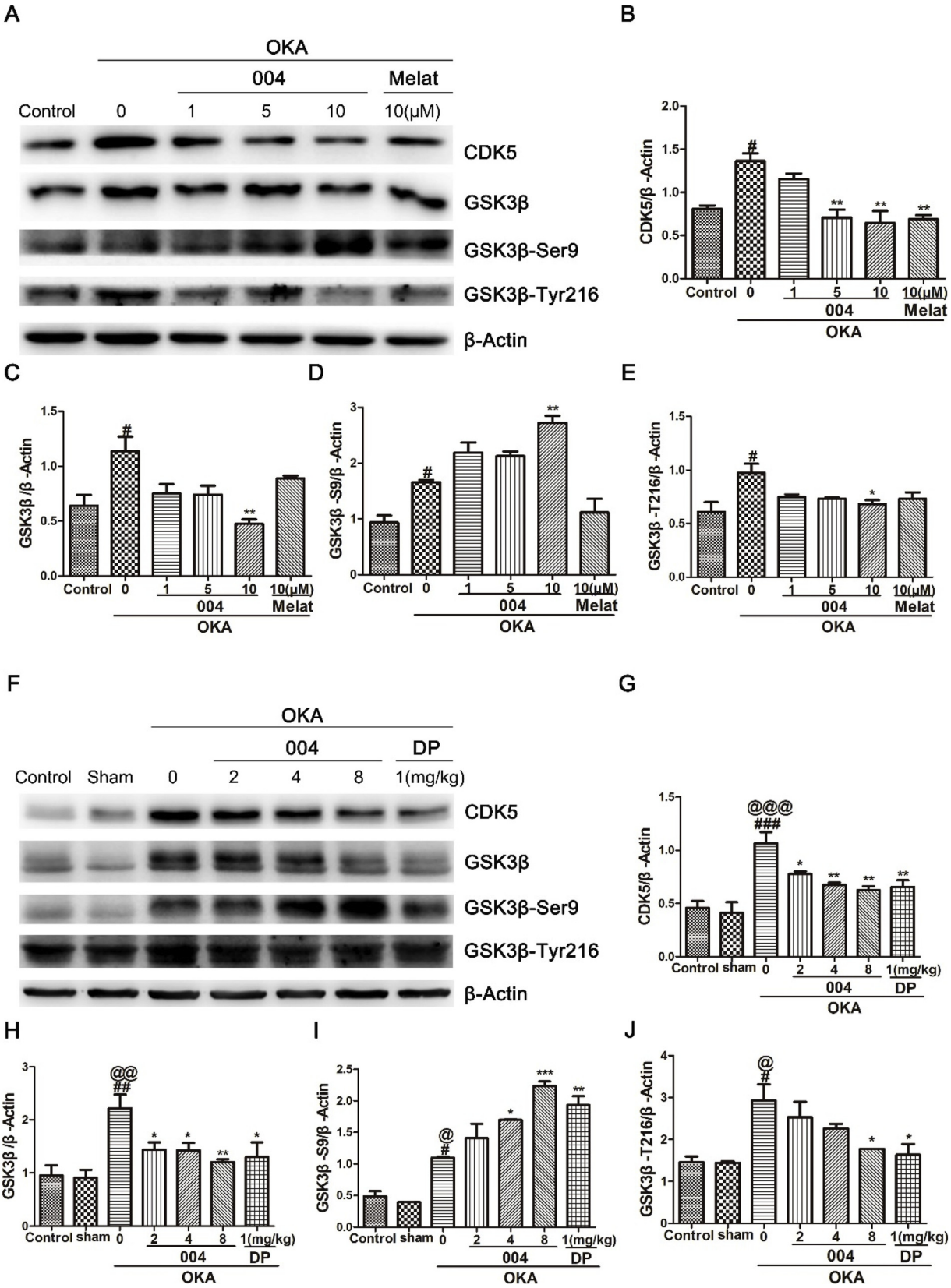

Fig. 8. 004 decreased the levels of CDK5 and GSK3β induced by OKA *in vitro* and *in vivo*. A and B: The level of CDK5 in PC12 cells; A and C: the level of GSK3β in PC12 cells; A and D: the level of P-GSK3β-S9 in PC12 cells; A and E: the level of P-GSK3β-T216 in PC12 cells; F and G: the level of CDK5 in rats; F and H: the level of GSK3β in rats; F and I: the level of P-GSK3β-S9 in rats; F and J: the level of P-GSK3β-T216 in rats. $^{\#}p < 0.05$, $^{\#\#}p < 0.01$ *vs*. the Control group; $^{@}p < 0.05$, $^{@@}p < 0.01$, $^{@@@}p < 0.001$ *vs*. the Sham group; $^{*}p < 0.05$, $^{**}p < 0.01$, $^{***}p < 0.001$ *vs*. the OKA group. Mean ± SEM in each group.

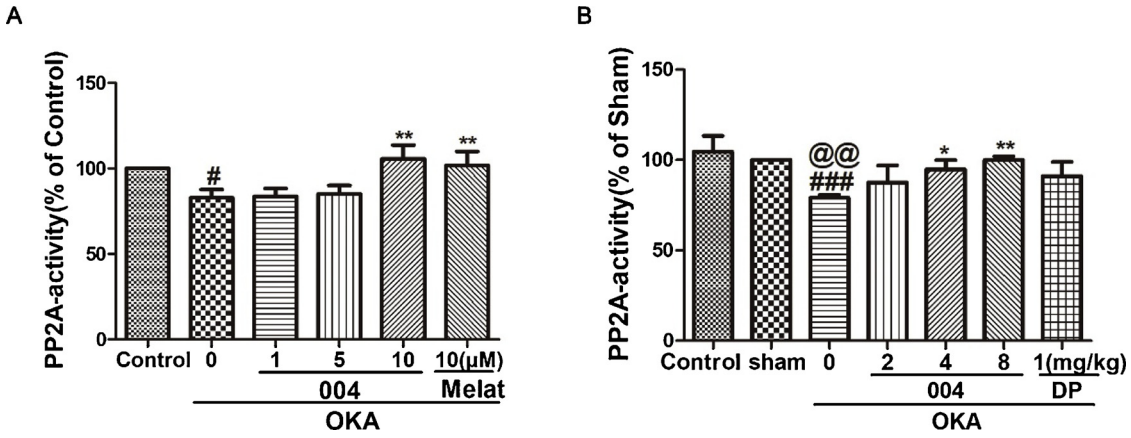

Fig. 9. 004 enhanced PP2A activity in the OKA-induced AD model *in vitro* and *in vivo*. A: PP2A activity in PC12 cells; B: PP2A activity in the right hippocampus of rats. $^{\#}p < 0.05$, $^{\#\#\#}p < 0.001$ *vs*. the Control group; $^{@@}p < 0.01$ *vs*. the Sham group; $^{*}p < 0.05$, $^{**}p < 0.01$ *vs*. the OKA group. Mean ± SD in each group, n = 3.

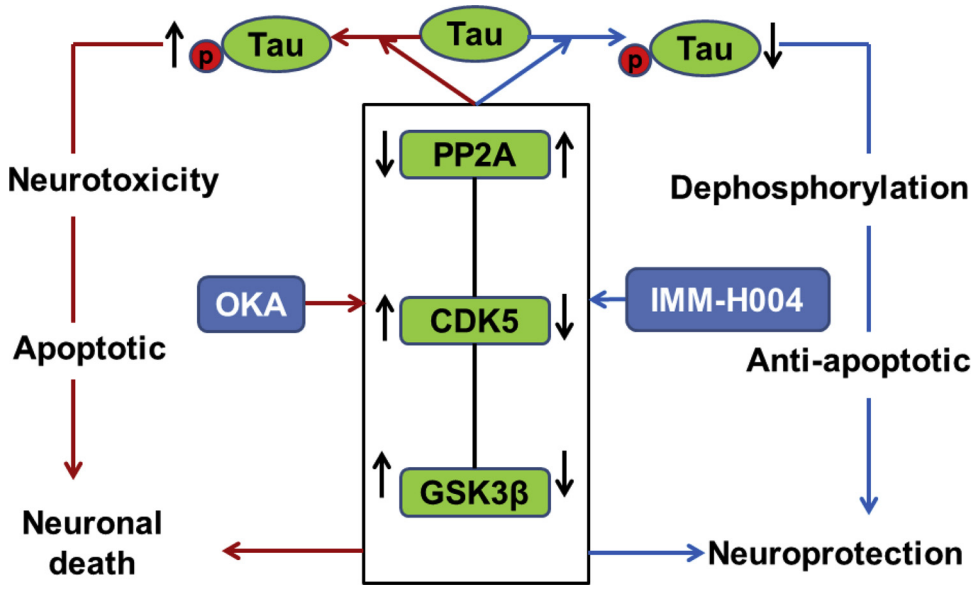

Fig. 10. A schematic of the effect of 004 in the OKA-induced AD-like model.

regulation of Tau phosphorylation and has been suggested to be involved in abnormal Tau phosphorylation and aggregation in AD. GSK3β can catalyze Tau protein phosphorylation at multiple sites (Spittaels et al., 2000; Wang et al., 2007). GSK3β activity is regulated by site-specific phosphorylation, and GSK3β activity is inhibited by its phosphorylation at S9 and Thr390 and activated by its phosphorylation at T216 (Cai et al., 2007; Chen et al., 2001; Goc et al., 2014; Hughes et al., 1993).

Therefore, on the basis of pharmacodynamics, we preliminarily explored the mechanism by which 004 suppresses OKA-induced AD-like degeneration. Taking PP2A, CDK5 and GSK3β as markers, we demonstrated that 004 protected PC12 cells and brains of SD rats by regulating Tau protein phosphorylation at sites S214, T231, T205 and T181 through regulating PP2A, CDK5 and GSK3β. We confirmed that 004 protected the central nervous system and suppressed the pathological changes in an AD model induced by OKA *in vitro* and *in vivo*.

It is well known that Tau protein kinases and phosphatases and Tau sites are involved in the progression of AD, and there is a complex relationship among PP2A, CDK5 and GSK3β (Geschwind, 2003; Simic et al., 2016; Wang et al., 2015). It has been observed that abnormal CDK5 activation contributes to the inhibition of GSK3β (Chu et al., 2016; Plattner et al., 2006). However, in old transgenic animals, CDK5 increases GSK3β activity (Spittaels et al., 2000). Crosstalk between GSK3β and PP2A may also contribute to Tau hyperphosphorylation in the AD brain. It was reported that decreased activity of PP2A might decrease GSK3β activity, which may produce a vicious cycle of further reduced PP2A and GSK3β activity, thus increasing Tau hyperphosphorylation in the rat brain; additionally, it was reported that the activity level of PP2A positively correlated with the level of GSK3β in the mouse brain (Chu et al., 2016; Wang et al., 2015). However, the roles of PP2A, CDK5 and GSK3β in Tau hyperphosphorylation are not fully explained, and whether a mutual relationship between these proteins exists remains to be explored. We do not understand how 004 might act in terms of the mutual relationship between these enzymes. Future experiments are needed to test the specific mechanism of 004.

In conclusion (Fig. 10), 004 significantly inhibited neuronal cells death and improved spatial memory impairment induced by OKA. The mechanisms were as follows: 004 reduced OKA-induced Tau phosphorylation by inhibiting PP2A and increasing the activity of CDK5 and GSK3β, thereby suppressing microtubule destabilization and neurofibrillary tangle formation. Our study provided evidences that 004 reduced AD-like degeneration through inhibition of Tau pathology. This study provided support for new drug research and further research into 004.

CRediT authorship contribution statement

Yingying Wang: Writing - original draft, Writing - review & editing, Investigation, Formal analysis. **Xiuyun Song:** Writing - review & editing, Conceptualization, Methodology. **Dandan Liu:** Investigation. **Yu-xia Lou:** Investigation. **Piao Luo:** Investigation. **Tianbi Zhu:** Investigation. **Qi Wang:** Conceptualization, Methodology, Funding acquisition. **Naihong Chen:** Conceptualization, Methodology, Funding acquisition.

Declaration of Competing Interest

The authors declare no conflict of interest.

Acknowledgments

This work was supported by the National Natural Science Foundation of China (81603315, 81603316, U1402221), CAMS Innovation Fund for Medical Sciences (CIFMS) (2016-I2M-1-004), Beijing Key Laboratory of New Drug Mechanisms and Pharmacological Evaluation Study (BZ0150), and Key Research and Development Project of Hunan Province (2015SK2029-1).

References

Alonso, A.D., Di Clerico, J., Li, B., Corbo, C.P., Alaniz, M.E., Grundke-Iqbal, I., Iqbal, K., 2010. Phosphorylation of tau at Thr212, Thr231, and Ser262 combined causes neurodegeneration. J. Biol. Chem. 285, 30851–30860.
Bialojan, C., Takai, A., 1988. Inhibitory effect of a marine-sponge toxin, okadaic acid, on protein phosphatases. Biochem. J. 256, 283–290.
Blennow, K., De Leon, M.J., Zetterberg, H., 2006. Alzheimer's disease. Lancet 368, 387–403.
Buée, L., Bussière, T., Buée-Scherrer, V., Delacourte, A., Hof, P.R., 2000. Tau protein isoforms, phosphorylation and role in neurodegenerative disorders. Brain Res. Brain Res. Rev. 33, 95–130.
Cai, G.Q., Wang, J., Xin, X.Y., Ke, Z.J., Luo, J., 2007. Phosphorylation of glycogen synthase kinase-3β at serine 9 confers cisplatin resistance in ovarian cancer cells. Int. J. Oncol. 31, 657–662.
Chen, E.Y., Mazure, N.M., Cooper, J.A., Giaccia, A.J., 2001. Hypoxia activates a platelet-derived growth factor receptor/phosphatidylinositol 3-kinase/Akt pathway that results in glycogen synthase kinase-3 inactivation. Cancer Res. 61, 2429–2433.
Chen, S., Cheng, A.C., Wang, M.S., Peng, X., 2008. Detection of apoptosis induced by new type gosling viral enteritis virus in vitro through fluorescein annexin V-FITC/PI double labeling. World J. Gastroenterol. 14, 2174–2178.
Chu, D., Tan, J., Xie, S., Jin, N., Yin, X., Gong, C.X., Iqbal, K., Liu, F., 2016. GSK-3beta is dephosphorylated by PP2A in a Leu309 methylation-independent manner. J. Alzheimers Dis. 49, 365–375.
Cruz, J.C., Tsai, L.H., 2004. Cdk5 deregulation in the pathogenesis of Alzheimer's disease. Trends Mol. Med. 10, 452–458.
Geschwind, D.H., 2003. Tau phosphorylation, tangles, and neurodegeneration: the chicken or the egg? Neuron 40, 457–460.
Goc, A., Al-Husein, B., Katsanevas, K., Steinbach, A., Lou, U., Sabbineni, H., DeRemer, D.L., Somanath, P.R., 2014. Targeting Src-mediated Tyr216 phosphorylation and activation of GSK-3 in prostate cancer cells inhibit prostate cancer progression in vitro and in vivo. Oncotarget 5, 775–787.
Gong, C.X., Lidsky, T., Wegiel, J., Zuck, L., Grundke-Iqbal, I., Iqbal, K., 2000. Phosphorylation of microtubule-associated protein tau is regulated by protein phosphatase 2A in mammalian brain. Implications for neurofibrillary degeneration in Alzheimer's disease. J. Biol. Chem. 275, 5535–5544.
Huang, G., Zhou, J., Zhan, W., Xiong, Y., Hu, C., Li, X., Li, X., Li, Y., et al., 2013. The neuroprotective effects of intraperitoneal injection of hydrogen in rabbits with cardiac arrest. Resuscitation 84, 690–695.
Hughes, K., Nikolakaki, E., Plyte, S.E., Totty, N.F., Woodgett, J.R., 1993. Modulation of the glycogen synthase kinase-3 family by tyrosine phosphorylation. EMBO J. 12, 803–808.
Kamat, P.K., Rai, S., Swarnkar, S., Shukla, R., Nath, C., 2014. Molecular and cellular mechanism of okadaic acid (OKA)-induced neurotoxicity: a novel tool for Alzheimer's disease therapeutic application. Mol. Neurobiol. 50, 852–865.
Kamat, P.K., Tota, S., Shukla, R., Ali, S., Najmi, A.K., Nath, C., 2011. Mitochondrial dysfunction: a crucial event in okadaic acid (ICV) induced memory impairment and apoptotic cell death in rat brain. Pharmacol. Biochem. Behav. 100, 311–319.
Kamat, P.K., Nath, C., 2015. Okadaic acid: a tool to study regulatory mechanisms for neurodegeneration and regeneration in Alzheimer's disease. Neural Regen. Res. 10, 365–367.
Liu, F., Li, B., Tung, E.J., Grundke-Iqbal, I., Iqbal, K., Gong, C.X., 2007. Site-specific effects of tau phosphorylation on its microtubule assembly activity and self-aggregation. Eur. J. Neurosci. 26, 3429–3436.
Liu, R., Wang, J.Z., 2009. Protein phosphatase 2A in Alzheimer's disease. Pathophysiology 16, 273–277.
Longin, S., Zwaenepoel, K., Louis, J.V., Dilworth, S., Goris, J., Janssens, V., 2007. Selection of protein phosphatase 2A regulatory subunits is mediated by the C terminus of the catalytic subunit. J. Biol. Chem. 282, 26971–26980.
Martin, L., Latypova, X., Wilson, C.M., Magnaudeix, A., Perrin, M.L., Terro, F., 2013. Tau protein phosphatases in Alzheimer's disease: the leading role of PP2A. Ageing Res. Rev. 12, 39–49.
Martin, L., Page, G., Terro, F., 2011. Tau phosphorylation and neuronal apoptosis induced by the blockade of PP2A preferentially involve GSK3beta. Neurochem. Int. 59, 235–250.
Martinez, A., Castro, A., Dorronsoro, I., Alonso, M., 2002. Glycogen synthase kinase 3 (GSK-3) inhibitors as new promising drugs for diabetes, neurodegeneration, cancer, and inflammation. Med. Res. Rev. 22, 373–384.
Medina, M., Avila, J., 2014. New perspectives on the role of tau in Alzheimer's disease. Implications for therapy. Biochem. Pharmacol. 88, 540–547.
Mo, S.T., Chiang, S.J., Lai, T.Y., Cheng, Y.L., Chung, C.E., Kuo, S.C., Reece, K.M., Chen, Y.C., et al., 2014. Visualization of subunit interactions and ternary complexes of protein phosphatase 2A in mammalian cells. PLoS One 9, e116074.
Noble, W., Olm, V., Takata, K., Casey, E., Mary, O., Meyerson, J., Gaynor, K., LaFrancois, J., et al., 2003. Cdk5 is a key factor in tau aggregation and tangle formation in vivo. Neuron 38, 555–565.
Plattner, F., Angelo, M., Giese, K.P., 2006. The roles of cyclin-dependent kinase 5 and glycogen synthase kinase 3 in tau hyperphosphorylation. J. Biol. Chem. 281, 25457–25465.
Qian, W., Shi, J., Yin, X., Iqbal, K., Grundke-Iqbal, I., Gong, C.X., Liu, F., 2010. PP2A regulates tau phosphorylation directly and also indirectly via activating GSK-3beta. J. Alzheimers Dis. 19, 1221–1229.
Reszka Krzysztof, J., Britigan Bradley, E., 2007. Doxorubicin inhibits oxidation of 2,2′-azino-bis(3-ethylbenzothiazoline-6-sulfonate) (ABTS) by a lactoperoxidase/H2O2 system by reacting with ABTS-derived radical. Arch. Biochem. Biophys. 466, 164–171.
Simic, G., Babic Leko, M., Wray, S., Harrington, C., Delalle, I., Jovanov-Milosevic, N., Bazadona, D., Buee, L., et al., 2016. Tau protein hyperphosphorylation and aggregation in Alzheimer's disease and other Tauopathies, and possible neuroprotective strategies. Biomolecules 6 (6).
Song, H., Kim, W., Choi, J.H., Kim, S.H., Lee, D., Park, C.H., Kim, S., Kim, D.Y., et al., 2016a. Stress-induced nuclear translocation of CDK5 suppresses neuronal death by downregulating ERK activation via VRK3 phosphorylation. Sci. Rep. 6, 28634.
Song, X.Y., Hu, J.F., Sun, M.N., Li, Z.P., Wu, D.H., Ji, H.J., Yuan, Y.H., Zhu, Z.X., et al., 2013. IMM-H004, a novel coumarin derivative compound, protects against amyloid beta-induced neurotoxicity through a mitochondrial-dependent pathway. Neuroscience 242, 28–38.
Song, X.Y., Wang, Y.Y., Chu, S.F., Hu, J.F., Yang, P.F., Zuo, W., Song, L.K., Zhang, S., et al., 2016b. A new coumarin derivative, IMM-H004, attenuates okadaic acid-induced spatial memory impairment in rats. Acta Pharmacol. Sin. 37, 444–452.
Spittaels, K., Van den Haute, C., Van Dorpe, J., Geerts, H., Mercken, M., Bruynseels, K., Lasrado, R., Vandezande, K., et al., 2000. Glycogen synthase kinase-3beta phosphorylates protein tau and rescues the axonopathy in the central nervous system of human four-repeat tau transgenic mice. J. Biol. Chem. 275, 41340–41349.
Stoiljkovic, M., Kelley, C., Horvath, T.L., Hajos, M., 2018. Neurophysiological signals as predictive translational biomarkers for Alzheimer's disease treatment: effects of donepezil on neuronal network oscillations in TgF344-AD rats. Alzheimers Res. Ther. 10, 105.
Tanaka, T., Zhong, J., Iqbal, K., Trenkner, E., Grundke-Iqbal, I., 1998. The regulation of phosphorylation of tau in SY5Y neuroblastoma cells: the role of protein phosphatases. FEBS Lett. 426, 248–254.
Tian, Q., Lin, Z.Q., Wang, X.C., Chen, J., Wang, Q., Gong, C.X., Wang, J.Z., 2004. Injection of okadaic acid into the meynert nucleus basalis of rat brain induces decreased acetylcholine level and spatial memory deficit. Neuroscience 126, 277–284.
Vermes, I., Haanen, C., Steffens-Nakken, H., Reutelingsperger, C., 1995. A novel assay for apoptosis. Flow cytometric detection of phosphatidylserine expression on early apoptotic cells using fluorescein labelled Annexin V. J. Immunol. Methods 184, 39–51.
Vorhees, C.V., Williams, M.T., 2006. Morris water maze: procedures for assessing spatial and related forms of learning and memory. Nat. Protoc. 1, 848–858.
Wagner, U., Utton, M., Gallo, J.M., Miller, C.C., 1996. Cellular phosphorylation of tau by GSK-3 beta influences tau binding to microtubules and microtubule organisation. J. Cell. Sci. 109, 1537–1543.
Wang, J.Z., Grundke-Iqbal, I., Iqbal, K., 2007. Kinases and phosphatases and Tau sites involved in Alzheimer neurofibrillary degeneration. Eur. J. Neurosci. 25, 59–68.
Wang, J.Z., Gong, C.X., Zaidi, T., Grundke-Iqbal, I., Iqbal, K., 1995. Dephosphorylation of Alzheimer paired helical filaments by protein phosphatase-2A and -2B. J. Biol. Chem. 270, 4854–4860.
Wang, J.Z., Grundke-Iqbal, I., Iqbal, K., 1996. Glycosylation of microtubule-associated protein Tau: an abnormal posttranslational modification in Alzheimer's disease. Nat. Med. 2, 871–875.
Wang, Y.Y., Song, X.Y., Wang, Q., Chen, N.H., 2016. The protective effects of Ginsenosides Rg1 in AD-like pathological model induced by okadaic acid. Chin. Pharmacol. Bull. 32, 1064–1070.
Wang, Y., Yang, R., Gu, J., Yin, X., Jin, N., Xie, S., Wang, Y., Chang, H., et al., 2015. Cross talk between PI3K-AKT-GSK-3beta and PP2A pathways determines tau hyperphosphorylation. Neurobiol. Aging 36, 188–200.
Wilkaniec, A., Czapski, G.A., Adamczyk, A., 2016. Cdk5 at crossroads of protein oligomerization in neurodegenerative diseases: facts and hypotheses. J. Neurochem. 136, 222–233.
Yang, C.C., Kuai, X.X., Gao, W.B., Yu, J.C., Wang, Q., Li, L., Zhang, L., 2016. Morroniside-

induced PP2A activation antagonizes Tau hyperphosphorylation in a cellular model of neurodegeneration. J. Alzheimers Dis. 51, 33–44.
Yoon, S., Choi, J., Yoon, J., Huh, J.W., Kim, D., 2006. Okadaic acid induces JNK activation, bim overexpression and mitochondrial dysfunction in cultured rat cortical neurons. Neurosci. Lett. 394, 190–195.
Zhao, Z., Bouchard, P., Diltz, C.D., Shen, S.H., Fischer, E.H., 1993. Purification and characterization of a protein tyrosine phosphatase containing SH2 domains. J. Biol. Chem. 268, 2816–2820.
Zheng, H., Niu, S., Zhao, H., Li, S., Jiao, J., 2018. Donepezil improves the cognitive impairment in a tree shrew model of Alzheimer's disease induced by amyloid-beta1-40 via activating the BDNF/TrkB signal pathway. Metab. Brain Dis. 33, 1961–1974.
Zhou, S., Yu, G., Chi, L., Zhu, J., Zhang, W., Zhang, Y., Zhang, L., 2013. Neuroprotective effects of edaravone on cognitive deficit, oxidative stress and tau hyperphosphorylation induced by intracerebroventricular streptozotocin in rats. Neurotoxicology 38, 136–145.